

# Hyperconnectivity Associated with Anosognosia Accelerating Clinical Progression in Amnesic Mild Cognitive Impairment

Shanshan Chen,<sup>#</sup> Yu Song,<sup>#</sup> Huimin Wu,<sup>#</sup> Honglin Ge, Wenzhang Qi, Yue Xi, Jiayi Wu, Yuxiang Ji, Kexin Chen, Xingjian Lin,<sup>\*</sup> and Jiu Chen<sup>\*</sup>



Cite This: <https://doi.org/10.1021/acchemneuro.1c00595>

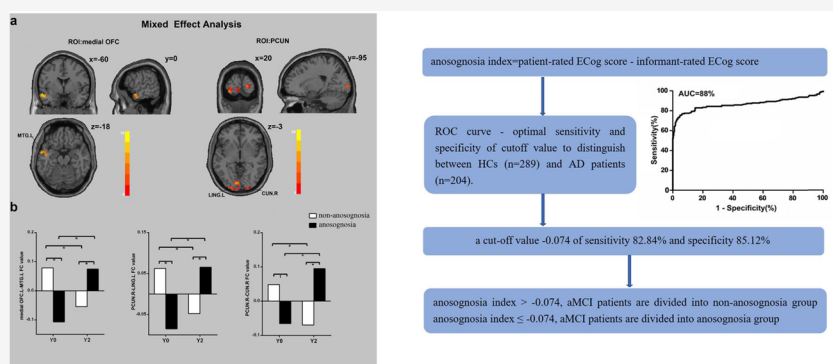


Read Online

ACCESS |

Metrics & More

Article Recommendations



**ABSTRACT:** The incidence and prevalence of anosognosia are highly variable in amnesic mild cognitive impairment (aMCI) patients. The study aims to explore the neuropathological mechanism of anosognosia in aMCI patients using two different but complementary technologies, including  $^{18}\text{F}$ -flortaucipir positron emission tomography and resting state functional magnetic resonance imaging. The study found that anosognosia was related to higher tau accumulation in the left medial orbitofrontal cortex (OFC), left posterior cingulate cortex, and right precuneus in aMCI patients. Intrinsic functional connectivity analyses found significant correlations between anosognosia index and hypoconnectivity between the left medial OFC and left middle temporal gyrus (MTG), right precuneus and left lingual gyrus. Longitudinally, the connectivity of these brain regions as well as the right precuneus and right cuneus showed hyperconnectivity in aMCI patients with anosognosia. The anosognosia index was also correlated with AD pathological markers (i.e.,  $A\beta$ , t-tau, and p-tau) and brain glucose metabolism in aMCI patients. In conclusion, anosognosia in aMCI patients is associated with the dysfunction of medial OFC-MTG circuit and the precuneus–visual cortex circuit and accelerates clinical progression to AD dementia.

**KEYWORDS:** Amnesic mild cognitive impairment, anosognosia, cognitive awareness, resting state functional magnetic resonance imaging, [ $^{18}\text{F}$ ]flortaucipir positron emission tomography,  $F^{18}$ -fluorodeoxyglucose positron emission tomography

## INTRODUCTION

Anosognosia is a symptom featured with a lack of knowledge of the patient's own disease state, and it can be observed in many diseases.<sup>1</sup> In the context of Alzheimer's disease (AD), anosognosia specifically refers to a deficiency of awareness of the presence or severity of cognitive deficits.<sup>2</sup> Amnesic mild cognitive impairment (aMCI), manifested as objective cognitive impairment dominated by memory decline without daily life impairment, is considered the prodementia stage of AD.<sup>3</sup> Anosognosia is a frequent symptom in AD patients, but its incidence and prevalence are highly variable in aMCI patients.<sup>4</sup> Studies indicated that anosognosia not only is correlated to disease severity but also independently predicts the conversion of aMCI to AD.<sup>5,6</sup> Therefore, paying attention

to the neural basis of anosognosia may be of great significance for revealing the progression mechanism of aMCI.

For the past few years, converged evidence from multiple neuroimaging technologies has shown that anosognosia in MCI/AD patients was associated with a wide range of abnormal function or morphological variables, including the prefrontal, temporopolar, hippocampus, parietal lobe, and subcortical regions.<sup>5,7–10</sup> Studies also exhibited the decreased

**Received:** September 8, 2021

**Accepted:** November 2, 2021

functional connectivity (FC) between prefrontal regions and medial temporal lobe (i.e., hippocampus), which is positively associated with anosognosia in MCI/AD patients.<sup>11,12</sup> Although studies have focused on the characteristics of FC changes, the results were inconsistent. A self-appraisal task study reported attenuated activity in the medial prefrontal cortex and posterior cingulate cortex, while another study reported intact activity in cortical midline structures compared to healthy controls (HCs).<sup>13,14</sup> The inconsistency of these results may be explained by some confounding factors. First, when compared to HC, the coexistence of cognitive impairment and anosognosia in MCI/AD patients may be a confounder because the impaired cognition may cover up the true relationship between anosognosia and the neurological basis. Second, the aforementioned studies regarding the MCI diagnostic group as a single entity and assumed all MCI patients were accompanied by anosognosia, regardless of the remarkable differences between individuals observed clinically, which may decrease the reliability of the obtained behavior–brain relationship. Therefore, it is essential to clarify intergroup variabilities related to anosognosia when investigating the neural basis of anosognosia in aMCI patients.

To address the aforementioned research gaps, we divided aMCI patients into two subgroups on the basis of whether they are accompanied by anosognosia, namely, aMCI with anosognosia group and aMCI with nonanosognosia group. The symptoms of anosognosia are determined by the anosognosia index, which is calculated by the difference score between parallel questionnaire for the participants and for their caregivers. This method was proven to be reliable and applicable to assess anosognosia/cognitive awareness in previous studies.<sup>13,15–18</sup> A previous study found that an aMCI group with anosognosia had glucose hypometabolism in the posterior cingulate cortex (PCC) compared with non-anosognosia group.<sup>6</sup> Tagai et al. reported lower regional cerebral blood flows (CBFs) in the prefrontal cortex and higher CBF in the parietal cortex in aMCI with anosognosia group than nonanosognosia group.<sup>19</sup> To our knowledge, the characteristics of FC changes remain blank in aMCI patients with and without anosognosia, and there is no exploration of their longitudinal connectivity alterations. Thus, we aimed to evaluate altered intrinsic connectivity between aMCI patients with anosognosia and nonanosognosia groups as well as HCs. Subsequently longitudinal FC trajectory was also explored in aMCI subgroups. In addition, longitudinal alterations in cognition, pathological markers of AD, and brain glucose metabolism were also explored among three groups.

The [<sup>18</sup>F]flortaucipir positron emission tomography (PET) can detect the spatial distribution of hyperphosphorylated tau *in vivo*, with high specificity and sensitivity for early detection of AD molecular pathological changes.<sup>20</sup> Functional magnetic resonance imaging (fMRI) is an advanced auxiliary technology that can detect structural changes reflecting microscopic neurons and their synapses. The brain function activity measured by fMRI and the tau standardized uptake value ratios (SUVRs) by [<sup>18</sup>F]flortaucipir PET play a role as a bridge linking the underlying molecular mechanism and the cognitive performance and are an important aspect of AD neuropathological mechanism. Here, we used the two different but complementary imaging modalities to reveal the underlying neuropathological mechanism of anosognosia in aMCI patients. First, we compared regional [<sup>18</sup>F]flortaucipir uptake between anosognosia and nonanosognosia groups to unravel

the higher tau deposition regions associated with anosognosia. Thereafter, high tau accumulation regions obtained above served as regions of seed for further intrinsic FC analyses to explore the abnormalities of FC in aMCI patients using resting state fMRI.

The purpose of this research is to study the neuroimaging characteristics and AD pathological markers changes at baseline and 2-year follow-up in aMCI patients with and without anosognosia using two different but complementary methods including PET and fMRI technology. Our main hypothesis is as follows: First, there exists a distinct FC alteration in aMCI patients with anosognosia at baseline, which may be associated with the severity of anosognosia. Then, there are unique FC trajectory changes in aMCI patients with anosognosia and nonanosognosia groups during the longitudinal follow-up. Finally, we hypothesize that aMCI patients with anosognosia have worse cognition, AD pathological markers, low brain metabolism, and accelerated clinical progression compared with the nonanosognosia group and HCs after 2-year follow-up.

## RESULTS AND DISCUSSION

To our knowledge, this is the first multimodal, longitudinal analysis of the neurological basis of anosognosia in aMCI patients. First, we found that aMCI patients with anosognosia had high tau accumulation in the left medial orbitofrontal cortex (OFC), left PCC, and right precuneus as compared to patients with nonanosognosia using [<sup>18</sup>F]flortaucipir PET. Second, using intrinsic connectivity analysis, we have replicated reduced intrinsic connectivity within the cortical midline structures and its connectivity with medial temporal lobe (i.e., MTG), which validates previous research.<sup>11,21</sup> We also reported novel findings that abnormal FC of the right precuneus and visual cortex was associated with anosognosia in aMCI patients. Further, longitudinal FC analysis found hyperconnectivity between left medial OFC and left MTG as well as right precuneus and bilateral visual cortex in aMCI with anosognosia. Third, the longitudinally deteriorating trajectory of cognition, AD pathological markers, and brain metabolism in aMCI patients with anosognosia compared with non-anosognosia patients suggested that anosognosia may accelerate disease progression. These findings are consistent with our previous hypothesis and emphasize the importance of anosognosia in the management of aMCI patients.

**Demographic and Neuropsychological Characteristics.** Seventy-seven subjects were enrolled in this study, including 25 HCs subjects, 22 aMCI patients with anosognosia, and 30 aMCI patients with nonanosognosia at baseline and 2-year follow-up. Briefly, there was no statistical discrepancy in the age ( $P = 0.290$ ), gender ( $P = 0.128$ ), and education level ( $P = 0.511$ ) among three groups. Memory function, executive function, anosognosia index, and brain metabolism among the three groups were statistically evident ( $P < 0.05$ ) at baseline and 2-year follow-up. Cerebrospinal fluid (CSF) total tau (t-tau) had no difference between the three groups in the baseline period, but it was found that aMCI with anosognosia group was significantly lower than nonanosognosia group after the 2-year follow-up. Although CSF amyloid  $\beta$ -protein ( $A\beta$ ) and CSF phosphorylated tau (p-tau) levels did not differ between aMCI subgroups and HCs subjects at baseline period, there was a tendency of pathological damage in aMCI with anosognosia. More details can be acquired from Table 1 and Figure 1.

**Table 1. Sociodemographic and Clinical Characteristics of HCs and aMCI with Nonanosognosia and Anosognosia Groups at Baseline and 2-Year Follow-Up Period<sup>a</sup>**

|  | HCs ( <i>n</i> = 25)         | nonanosognosia group ( <i>n</i> = 30) | anosognosia group ( <i>n</i> = 22) | <i>F</i> / $\chi^2$ | <i>p</i> -value |
|--|------------------------------|---------------------------------------|------------------------------------|---------------------|-----------------|
| Age (years)                            | 72.06 ± 6.04                 | 69.92 ± 6.84                          | 72.63 ± 6.95                       | 1.25                | 0.290           |
| Gender (F/M)                           | 10/15                        | 18/12                                 | 15/7                               | 4.11                | 0.128           |
| Education (years)                      | 16.4 ± 2.18                  | 16.4 ± 2.91                           | 15.64 ± 2.57                       | 0.68                | 0.511           |
| <b>MoCA</b>                            |                              |                                       |                                    |                     |                 |
| Y0                                     | 25.76 ± 2.26 <sup>ab</sup>   | 23.77 ± 3.37                          | 23.36 ± 2.55                       | 5.10                | 0.008           |
| Y2                                     | 26.84 ± 2.09 <sup>ab</sup>   | 23.97 ± 3.74                          | 21.77 ± 4.80                       | 11.35               | <0.001          |
| <b>Memory function</b>                 |                              |                                       |                                    |                     |                 |
| Y0                                     | 1.01 ± 0.45 <sup>ab</sup>    | 0.37 ± 0.62                           | 0.23 ± 0.64                        | 12.99               | <0.001          |
| Y2                                     | 1.26 ± 0.39 <sup>ab</sup>    | 0.40 ± 0.80                           | −0.03 ± 0.92                       | 17.97               | <0.001          |
| <b>Executive function</b>              |                              |                                       |                                    |                     |                 |
| Y0                                     | 1.04 ± 0.56 <sup>a</sup>     | 0.75 ± 0.82                           | 0.32 ± 0.86                        | 5.38                | 0.007           |
| Y2                                     | 1.04 ± 0.56 <sup>a</sup>     | 0.76 ± 0.95 <sup>a</sup>              | 0.02 ± 1.06                        | 8.06                | 0.001           |
| <b>CSF A<math>\beta</math> (Y0/Y2)</b> |                              |                                       |                                    |                     |                 |
| Y0                                     | 1245.57 ± 450.00             | 1130.41 ± 433                         | 946.76 ± 420.95                    | 2.05                | 0.137           |
| Y2                                     | 1214.03 ± 499.19             | 1085.04 ± 467.20                      | 827.93 ± 479.33                    | 2.05                | 0.141           |
| <b>CSF t-tau (Y0/Y2)</b>               |                              |                                       |                                    |                     |                 |
| Y0                                     | 269.17 ± 92.67               | 267.83 ± 110.09                       | 343.27 ± 152.76                    | 2.44                | 0.096           |
| Y2                                     | 283.55 ± 116.52 <sup>t</sup> | 285.01 ± 101.18 <sup>a</sup>          | 396.23 ± 165.04                    | 3.59                | 0.036           |
| <b>CSF p-tau (Y0/Y2)</b>               |                              |                                       |                                    |                     |                 |
| Y0                                     | 25.30 ± 10.16                | 24.96 ± 11.79 <sup>t</sup>            | 34.40 ± 18.25                      | 2.94                | 0.060           |
| Y2                                     | 27.40 ± 13.43                | 26.57 ± 10.53 <sup>t</sup>            | 39.00 ± 19.56                      | 3.31                | 0.051           |
| <b>FDG (Y0/Y2)</b>                     |                              |                                       |                                    |                     |                 |
| Y0                                     | 1.35 ± 0.08 <sup>a</sup>     | 1.30 ± 0.09                           | 1.26 ± 0.12                        | 4.82                | 0.011           |
| Y2                                     | 1.31 ± 0.08 <sup>a</sup>     | 1.31 ± 0.12 <sup>a</sup>              | 1.17 ± 0.13                        | 7.76                | 0.001           |
| <b>Cognitive awareness index</b>       |                              |                                       |                                    |                     |                 |
| Y0                                     | 0.13 ± 0.18 <sup>ab</sup>    | 0.47 ± 0.40 <sup>a</sup>              | −0.68 ± 0.53                       | 56.11               | <0.001          |
| Y2                                     | 0.26 ± 0.37 <sup>a</sup>     | 0.41 ± 0.55 <sup>a</sup>              | −0.89 ± 0.85                       | 32.82               | <0.001          |
| Conversion (%)                         | 0 (0.00) <sup>a</sup>        | 1 (3.33) <sup>a</sup>                 | 9 (40.91)                          | 21.38               | <0.001          |

<sup>a</sup>Numbers are given as means (standard deviation, SD) unless stated otherwise. The baseline sociodemographic and clinical characteristics of three comparisons were evaluated by ANOVA test and chi-square test, and posthoc test was obtained by Bonferroni corrected. <sup>ab</sup>There was statistical significance in comparison to aMCI patients with anosognosia after post hoc analysis, *P* < 0.05. <sup>b</sup>There was statistical significance in comparison to aMCI patients with nonanosognosia after post hoc analysis, *P* < 0.05, <sup>t</sup>*P* < 0.1. Abbreviations: MoCA, Montreal Cognitive Assessment; HCs, healthy controls; CSF, cerebrospinal fluid; A $\beta$ , amyloid  $\beta$ -protein; t-tau, total Tau; p-tau, phosphorylated tau; FDG, F18-fluorodeoxyglucose; Y0, baseline time; Y2, 2-year followed-up.

**Longitudinal Trajectories of Cognition, AD Pathological Markers, and Brain Metabolism.** Longitudinally, repeated measures analysis in the aMCI subgroups indicated that Montreal Cognitive Assessment (MoCA) and memory function showed significant group-time interaction effects, and executive function presented a marginal difference (Table 2). In addition, repeated measures of analysis of variance (ANOVA) revealed that CSF A $\beta$ , CSF t-tau, CSF p-tau, glucose metabolism, and anosognosia index among three groups were not significant in group-time interaction. Age, gender, and education level were controlled in all these repeated measures analysis. During the 2-year follow-up, 9 (40.91%) aMCI patients with anosognosia and 1 (3.33%) aMCI patient with nonanosognosia converted to AD dementia. More details can be seen in Table 2.

Cognitive decline complaints are considered as a requirement for the aMCI diagnosis. However, many studies found that as people age, the reliability of estimates of one's own cognitive abilities gradually declines.<sup>22,23</sup> Combining information provided by caregivers and participants has repeatedly proven to be highly accurate in many studies and has great clinical practical significance.<sup>15,24,25</sup> In our study, though there was no statistical difference between the aMCI with anosognosia and nonanosognosia groups at baseline, a faster

decline of global cognition, memory function, and executive function was observed in the anosognosia group during the follow-up period. The results indicated that the anosognosia may predict faster cognitive decline in aMCI patients, which agrees with the consensus from a previous study.<sup>6</sup> Munro et al. found that the progressor-MCI group had significantly lower anosognosia index than that of stable-MCI group, also supporting our results.<sup>26</sup> In addition, our study found that aMCI with anosognosia had more severe CSF t-tau, CSF p-tau, glucose hypometabolism, and faster clinical progression to AD dementia at the 2-year follow-up. The results were validated by a previous longitudinal clinical-pathological cohort study involving 2092 elderly people, reporting that the severity of anosognosia were associated with tau protein tangles in 385 patients who died and underwent neuropathological examination.<sup>25</sup> This study also verified another result from a pathological point of view; that is, CSF t-tau and CSF p-tau are negatively correlated with the anosognosia index in aMCI patients. Gerretsen and colleagues reported that anosognosia in aMCI patients is related to brain glucose hypometabolism, suggesting that anosognosia may be a valuable marker for the conversion of aMCI to AD.<sup>5</sup> However, the sample size of our study is small, and future large-scale longitudinal studies are

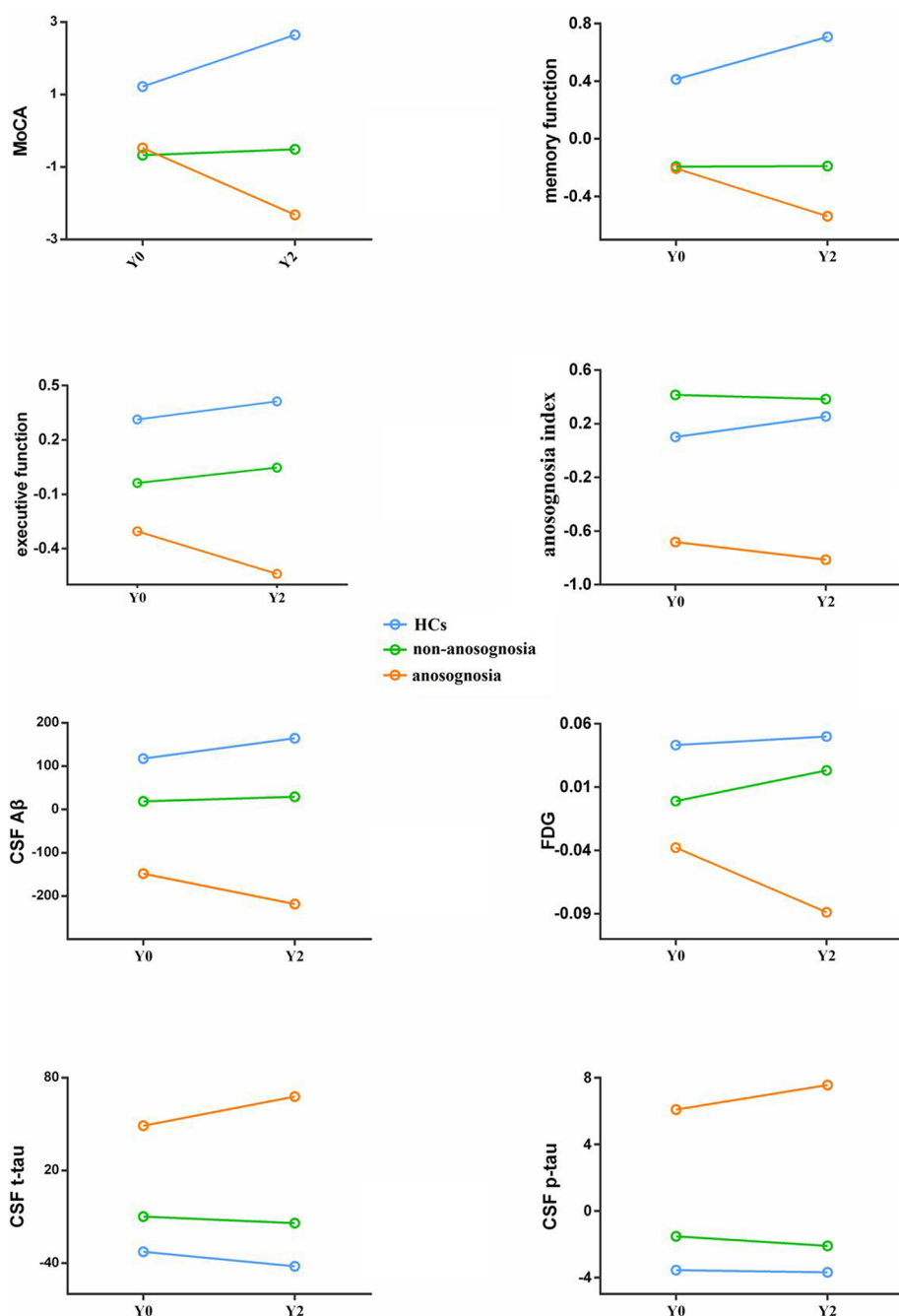


**Figure 1.** Mean cognition scores, pathological markers of AD, and FDG between groups at baseline and 2-year follow-up (adjusted for age, gender, and education level). Abbreviations: MoCA, Montreal Cognitive Assessment; HCs, healthy controls; CSF, cerebrospinal fluid; A $\beta$ , amyloid  $\beta$ -protein; t-tau, total tau; p-tau, phosphorylated tau; FDG, F<sup>18</sup>-fluorodeoxyglucose.

expected to reveal the correlativity between neuropathology and anosognosia in the AD continuum.

**Tau Accumulation Correlates of Anosognosia in aMCI Patients Using [<sup>18</sup>F]Flortaucipir PET.** Tau SUVRs in left medial OFC, left PCC, right precuneus, left caudal middle frontal, left frontal pole, left rostral middle frontal, and left parstriangularis showed significant differences between aMCI with anosognosia and nonanosognosia groups. Then, negative correlations between the anosognosia index and tau accumulation of the left medial OFC, the left PCC, and the right precuneus were observed in aMCI with anosognosia (medial OFC,  $r = -0.478$ ,  $P = 0.045$ ; PCC,  $r = -0.521$ ,  $P = 0.027$ ; precuneus,  $r = -0.550$ ,  $P = 0.018$ ). Thus, higher [<sup>18</sup>F]-

flortaucipir uptake in the left medial OFC, left PCC, and right precuneus in aMCI patients with anosognosia was correlated with the severity of anosognosia. The results support the connection between the medial OFC, PCC, and precuneus with anosognosia in aMCI, which was also consistent with abundant literature that reported the involvement of medial OFC, PCC, and precuneus in awareness or metacognitive processes.<sup>4,11,27,28</sup>

The medial OFC has been a common finding related with anosognosia in previous studies using various methods including SPECT, F<sup>18</sup>-fluorodeoxyglucose positron emission tomography (FDG-PET), and fMRI.<sup>7,11,29</sup> The medial OFC is situated in the foremost region of the cerebral cortex and is

**Table 2. Time Effects and Group-by-Time Interaction for Significance between aMCI with Anosognosia and Nonanosognosia Groups<sup>a</sup>**

|                    | time  |                    | group-time |                    |
|--------------------|-------|--------------------|------------|--------------------|
|                    | F     | P                  | F          | P                  |
| MoCA               | 4.046 | 0.050 <sup>t</sup> | 5.782      | 0.020 <sup>a</sup> |
| memory function    | 6.587 | 0.013 <sup>a</sup> | 6.869      | 0.013 <sup>a</sup> |
| executive function | 0.755 | 0.389              | 3.430      | 0.070 <sup>t</sup> |
| CSF A $\beta$      | 0.019 | 0.891              | 0.403      | 0.530              |
| CSF t-tau          | 1.338 | 0.256              | 0.054      | 0.818              |
| CSF p-tau          | 2.112 | 0.156              | 0.016      | 0.901              |
| anosognosia index  | 2.475 | 0.122              | 0.602      | 0.442              |
| FDG                | 0.036 | 0.851              | 1.152      | 0.292              |

<sup>a</sup>Statistical significance: <sup>a</sup>P < 0.05; <sup>t</sup>P < 0.1. Abbreviations: MoCA, Montreal Cognitive Assessment; HCs, healthy controls; CSF, cerebrospinal fluid; A $\beta$ , amyloid  $\beta$ -protein; t-tau, total tau; p-tau, phosphorylated tau; FDG, F<sup>18</sup>-fluorodeoxyglucose.

considered to participate in a wide range of cognitive activities, including planning, temporal processing, attention, behavioral flexibility, goal-directing, and emotional behaviors.<sup>30</sup> In the research on anosognosia, they found that the activation of medial OFC acts in the role of integrating current information with immediate past and regulating the gateway influenced by the changed internal and external demands.<sup>31,32</sup> The PCC is an important region of the default mode network, which has amyloid deposition and low glucose metabolism in the early stages of AD, and the change in its connectivity is reported as a predictor of AD conversion.<sup>33</sup> In the anosognosia section, PCC was reported to play a role in maintaining awareness and monitoring new intelligence, as well as self-knowledge retrieval for comparison and evaluation purpose.<sup>12,34</sup> In comparison, the participation of the precuneus has been infrequently elaborated in AD/MCI with anosognosia using neuroimaging technology.<sup>7</sup> The precuneus plays a central role in a wide spectrum of highly integrated tasks, including visuospatial function, episodic memory retrieval, and self-processing.<sup>35,36</sup> Tau aggregation of the precuneus in aMCI with anosognosia provided evidence that anosognosia is partly due to the failure to retrieve and manipulate autobiographical episodic memories.<sup>7,37</sup> In fact, the medial OFC, PCC, and precuneus brain areas as well as the medial parietal cortex and the retrosplenial cortex all belong to the cortical midline structures which serve as an anatomic and functional unit.<sup>38</sup> The cortical midline structures is the neural basis of self-referential processing to generate self-models.<sup>39</sup> The role of the cortical midline structures in the self-referential processing is integrating the internal self with the received external information to function as representation, monitoring, evaluation, and integration.<sup>40</sup> The continuous integration of internal and external stimuli from distinct domains forms the core self and then forms an experience with self as a unit.<sup>41</sup> In summary, our results verify the key role of the medial OFC, the PCC, and the precuneus in the metacognitive process of aMCI patients from histopathological mechanisms using [<sup>18</sup>F]flortaucipir PET.

**Intrinsic Connectivity Correlates of Anosognosia in aMCI Patients Using fMRI.** Three 6 mm spherical regions of interest centered in the medial OFC (MNI space of -6, 52, -19), left PCC (MNI space of -6, -38, 30), and right precuneus (MNI space of 9, -58, 39) obtained from tau PET analysis were created to perform intrinsic connectivity analyses on the three groups. In the FC map with left medial OFC as

the seed, the ANOVA analysis showed three significantly altered areas among the groups, including left middle temporal gyrus (MTG), right middle frontal gyrus (MFG), and right putamen (GRF-corrected *p*-value of <0.05, cluster size of >60 voxels, and two-tailed test). Compared to the HC, the aMCI with nonanosognosia group showed significantly increased FC in the right putamen and right MFG (GRF-corrected *p*-value of <0.01, cluster size of >30 voxels, and two-tailed test). Compared to the aMCI with nonanosognosia, the aMCI with anosognosia showed decreased FC in the left MTG. In the FC map with left PCC as the seed, the ANOVA analysis showed significantly altered regions in right orbital part of superior frontal gyrus among the three groups. Compared to the HC, the aMCI with anosognosia group showed significantly decreased FC in the right orbital part of superior frontal gyrus. In the FC map with the right precuneus as the seed, the ANOVA analysis showed significantly altered regions in bilateral lingual gyrus among the three groups. Compared to the aMCI with nonanosognosia group, the aMCI with anosognosia group showed significantly decreased FC in the left lingual gyrus. All results are controlling the effects of age, gender, education level, and GM volumes (see Figure 2 and Table 3).

Using the resting state fMRI, we found that anosognosia was also related to the altered FC of the medial OFC, PCC, precuneus, the MTG, and the visual cortex (i.e, lingual gyrus and cuneus). Compared with the aMCI with nonanosognosia group, anosognosia group had hypoconnectivity between left medial OFC and left MTG, as well as right precuneus and left lingual gyrus at baseline. The decreased FC between OFC and MTG was consistent with previous studies that anosognosia was due to the interruption of the FC between the self-related brain regions and the memory-related brain regions.<sup>7,11</sup> The results are also supported by the anatomical basis of the medial OFC–hippocampus circuit, which allows medial OFC to connect with the hippocampus and plays a key role in the consolidation of episodic memory.<sup>42</sup> On the basis of structural and functional relevance of anosognosia, the cognitive awareness model proposed by Antoine et al. provides a neurocognitive basis to account for the anosognosia.<sup>12</sup> In this model, the autobiographical memory system is linked to a personal database based on lifelong knowledge. The comparison of autobiographical memory and updated cognitive level in personal databases is a necessary condition for reflecting and evaluating the current cognitive changes to form an accurate self-awareness. Thus, when the cognitive impairment information cannot be uploaded and encoded into the autobiographical memory, patients suffer from anosognosia. In addition, our findings also revealed the decreased FC between precuneus and lingual gyrus in aMCI with the anosognosia group compared with the nonanosognosia group, which was less reported in previous studies. The lingual gyrus participates in visuospatial processing and visual memory, and it also plays an important role in divergent thinking by modulating the function of posterior regions including temporal, occipital, and parietal regions.<sup>43,44</sup> In a task fMRI study, the lingual gyrus was less activated in MCI patients than HCs during self-referential processing, suggesting it has been associated with self-related processes.<sup>14</sup> Compared with HCs, the reduction of GM volume in the lingual gyrus is related to the severity of anosognosia in mild AD patients, which also supports our findings.<sup>8</sup> In brief, our neuroimaging findings of decreased FC between precuneus and lingual gyrus prompted

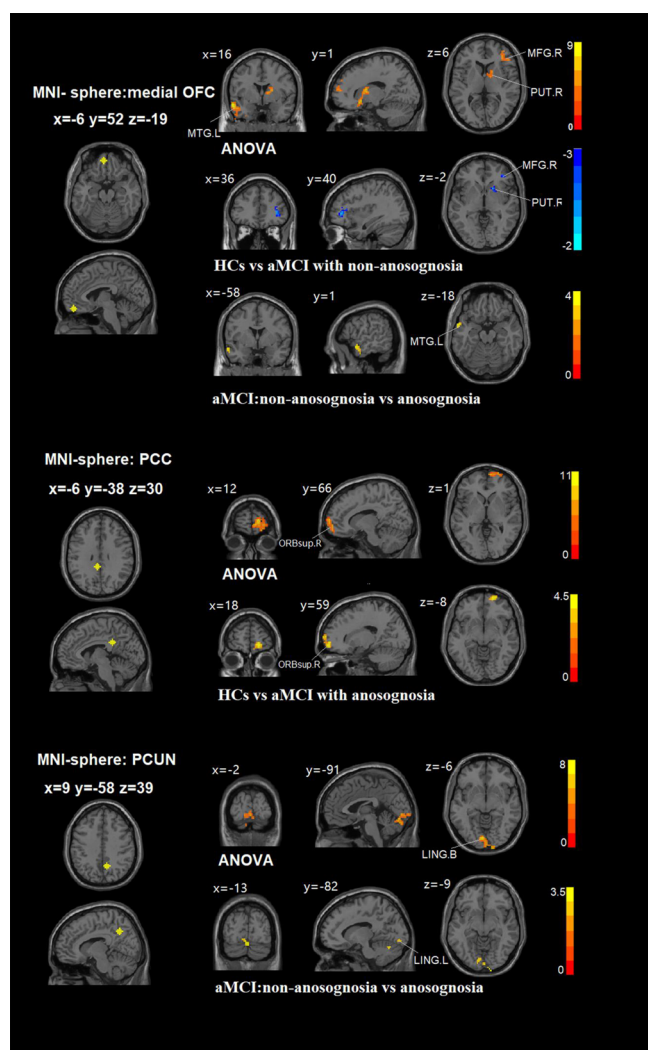


**Figure 2.** Functional connectivity differences of seed-based connectivity in HCs and aMCI with anosognosia and nonanosognosia groups. A GRF-corrected  $p$ -value of  $<0.05$ , a cluster size of  $>60$  voxels, and a two-tailed test were set for ANOVA analysis. A GRF-corrected  $p$ -value of  $<0.01$ , a cluster size of  $>30$  voxels, and a two-tailed test were set for post hoc comparisons. All results are controlling the effects of age, gender, education level, and gray matter volumes. Abbreviations: Medial OFC, medial orbitofrontal cortex; MTG, middle temporal gyrus; PCC, posterior cingulate cortex; MFG, middle frontal gyrus; PUT, putamen; ORBsup, orbital part of superior frontal gyrus; PCUN, precuneus; LING, lingual gyrus; HCs, healthy controls; aMCI, amnesic mild cognitive impairment; L, left; R, right; B, bilateral.

us to explore the neural mechanisms of the visual cortex involved in anosognosia in AD continuum.

Compared with the HCs, increased FC between the medial OFC and right putamen as well as right MFG was found in aMCI with the nonanosognosia group while hypoconnectivity between left PCC and right superior frontal gyrus was observed in aMCI with the anosognosia group. The increased FC between the medial OFC and putamen as well as MFG may be an increased engagement of neurons to withstand anosognosia. The putamen is the structure of the basal ganglia and is mainly involved in motor control.<sup>45</sup> It also participates in language and cognitive functions through a complex cortical-basal ganglia network.<sup>46</sup> Our results were supported by an FDG-PET study, which found that aMCI patients with

**Table 3. Intrinsic Connectivity Results Based on Seed-Based Analyses among Three Groups at Baseline<sup>a</sup>**

| region (aal)   | MNI coordinate |      |     | F/t   | cluster number |
|--|----------------|------|-----|-------|----------------|
|  | x              | y    | z   |       |                |
| Medial OFC Seed  |                |      |     |       |                |
| <b>ANOVA</b>   |                |      |     |       |                |
| L middle temporal gyrus                                  | -57            | 0    | -18 | 8.87  | 339            |
| R putamen  | 18             | 6    | 15  | 7.67  | 211            |
| R middle frontal gyrus                                   | 36             | 42   | 0   | 7.03  | 207            |
| <b>HCs &lt; aMCI with nonanosognosia</b>                 |                |      |     |       |                |
| R middle temporal gyrus                                  | 36             | 42   | 3   | -3.51 | 51             |
| R putamen  | 18             | 15   | -3  | -3.50 | 35             |
| <b>aMCI: nonanosognosia group &gt; anosognosia group</b> |                |      |     |       |                |
| L middle temporal gyrus                                  | -60            | 3    | -18 | 3.73  | 32             |
| PCC Seed   |                |      |     |       |                |
| <b>ANOVA</b>   |                |      |     |       |                |
| R superior frontal gyrus                                 | 18             | 60   | -6  | 10.69 | 200            |
| <b>HCs &gt; aMCI with anosognosia</b>                    |                |      |     |       |                |
| R superior frontal gyrus                                 | 18             | 60   | -6  | 4.60  | 99             |
| Precuneus Seed   |                |      |     |       |                |
| <b>ANOVA</b>   |                |      |     |       |                |
| B lingual gyrus  | 15             | -102 | 0   | 7.93  | 267            |
| <b>aMCI: nonanosognosia group &gt; anosognosia group</b> |                |      |     |       |                |
| L lingual gyrus  | -3             | -78  | -15 | 3.50  | 93             |

<sup>a</sup>A GRF-corrected  $p$ -value of  $<0.05$ , a cluster size of  $>60$  voxels, and a two-tailed test were set for ANOVA analysis. A GRF-corrected  $p$ -value of  $<0.01$ , a cluster size of  $>30$  voxels, and a two-tailed test were set for post hoc comparisons. All results are controlling the effects of age, gender, education level, and gray matter volumes. Abbreviations: HCs, healthy controls; aMCI, amnesic mild cognitive impairment; L, left; R, right; B, bilateral.

anosognosia had decreased brain metabolism in the basal forebrain as compared to the nonanosognosia group.<sup>6</sup> The abnormal activity of the putamen in aMCI patients with anosognosia suggests that there may be a link between the basal ganglia and anosognosia. Studies reported that the MFG mediates response selection and monitoring in contextual memory retrieval and is involved in the acquisition and representation of contingency awareness.<sup>47,48</sup> The hyperconnectivity between the left medial OFC and right MFG in nonanosognosia group compared with HCs can be a compensatory mechanism in the early stages of the disease to mobilize the relative number of surviving synapses to maintain cognitive self-awareness.<sup>49</sup> The decreased spontaneous brain activity in superior frontal gyrus has been observed in AD/MCI patients with anosognosia in previous studies.<sup>8,50</sup> In our study, the decreased connectivity between left PCC and right superior frontal gyrus validated the connection between superior frontal gyrus and awareness in aMCI patients.

**Longitudinal FC Correlates of Anosognosia in aMCI Patients Using fMRI.** We performed mixed effect analysis to explore the longitudinal alteration of FC between aMCI patients with anosognosia and nonanosognosia (GRF-corrected  $p$ -value of  $<0.01$ , cluster size of  $>60$ , two-tailed test). FC between left medial OFC and left MTG showed a group by time interaction: longitudinal decreased FC in aMCI with nonanosognosia, while longitudinal increased FC in aMCI with anosognosia. FC between the right precuneus and left lingual gyrus showed a group by time interaction: longitudinal decreased FC in aMCI with nonanosognosia, while longitudinal increased FC in aMCI with anosognosia. FC between

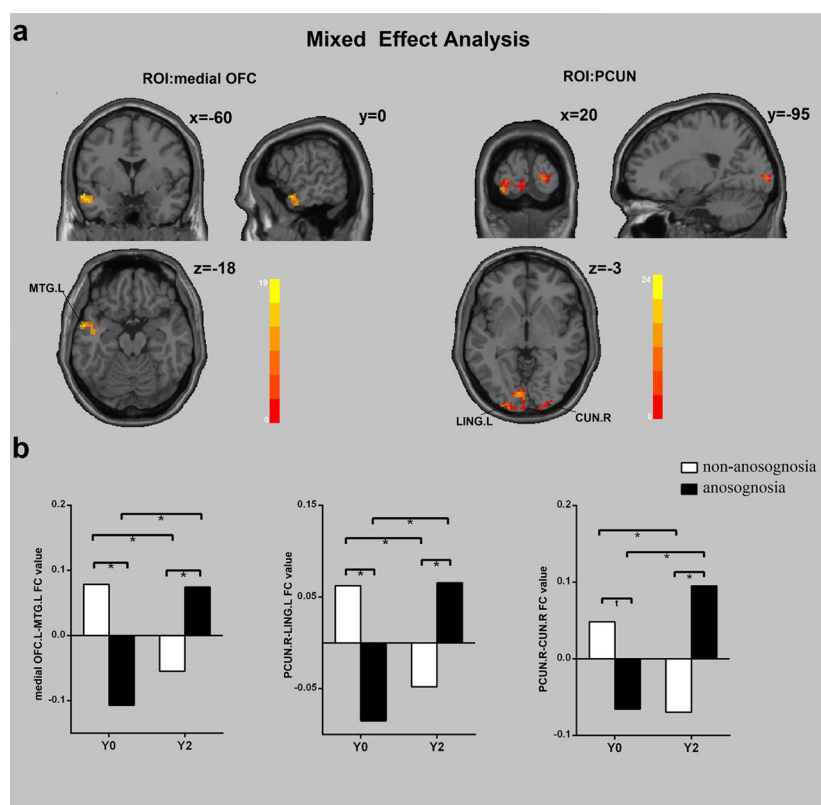


**Figure 3.** (a) Mixed effect analysis of seed-based connectivity patterns in aMCI with anosognosia and nonanosognosia groups. A GRF-corrected  $p$ -value of  $<0.01$ , a cluster size of  $>60$  voxels, and a two-tailed test were set for mixed effect analysis. All results are controlling the effects of age, gender, education level, and gray matter volumes. (b) Functional connectivity between left medial OFC and left MTG, right PCUN and left LING, right PCUN and right CUN showed a group by time interaction; \* statistical significance,  $P < 0.05$ ; t trend,  $P < 0.1$ . Abbreviations: Medial OFC, medial orbitofrontal cortex; MTG, middle temporal gyrus; PCUN, precuneus; LING, lingual gyrus; CUN, cuneus; L, left; R, right; B, bilateral; Y0, baseline time; Y2, 2-year follow-up.

right precuneus and right cuneus showed a group by time interaction: longitudinal decreased FC in aMCI with non-anosognosia, while longitudinal increased FC in aMCI with anosognosia. All results are after controlling the effects of age, gender, and education level (see Figure 3 and Table 4).

The mixed effects analyses found the intrinsic activities of left medial OFC and left MTG, right precuneus and left lingual gyrus, as well as right precuneus and right cuneus were longitudinally increased in aMCI with the anosognosia group while decreased in the nonanosognosia group after a 2-year follow-up. This pattern resembles a previously proposed

**Table 4. Mixed Effect Analysis of Seed-Based Connectivity in aMCI with Nonanosognosia and Anosognosia Groups<sup>a</sup>**

| region (aal)                            | MNI coordinate |     |     | F/t   | cluster number |
|---|----------------|-----|-----|-------|----------------|
|   | x              | y   | z   |       |                |
| <b>Medial orbitofrontal cortex seed</b> |                |     |     |       |                |
| L middle temporal gyrus                 | -60            | 0   | -18 | 19.79 | 105            |
| <b>Precuneus seed</b>                   |                |     |     |       |                |
| L lingual gyrus                         | -12            | -87 | -6  | 21.31 | 155            |
| R cuneus                                | 18             | -96 | 3   | 15.62 | 61             |

<sup>a</sup>A GRF-corrected  $p$ -value of  $<0.01$ , a cluster size of  $>60$  voxels, and a two-tailed test were set for mixed effect analysis. All results are controlling the effects of age, gender, education level, and gray matter volumes. Abbreviations: L, left; R, right; B, bilateral; MNI, Montreal Neurological Institute.

reverse “X” form model, in which a higher synchronization value is related to the progression of AD, while the opposite pattern may be related to a stable diagnosis of MCI; thus the hypersynchrony predicts subsequent network breakdown and disease conversion.<sup>51</sup> Research explained that the hypersynchrony is the consequence of the deposition of pathological markers, which leads to the surge of cortical neurotransmitters and the exhausting utilization of brain resources.<sup>52</sup> With the depletion of neurotransmitters and brain resources, there will be a rapid decline in cognition and accelerated disease progression.<sup>53</sup> In our results, higher synchronization values accompanied by lower cognitive scores and severe AD pathological markers (i.e., CSF  $A\beta$ , p-tau, t-tau) in the anosognosia group compared with the nonanosognosia group were consistent with the model, implying that anosognosia may represent a higher risk of conversion to dementia in a relatively short period of time. In short, the present work provides a new longitudinal evolution “X” model of hypersynchronization about anosognosia and a novel perspective for the future study of the neuropathological mechanism of anosognosia in AD continuum.

**Behavioral Implications of the Disordered FC and AD Biomarkers.** Pearson correlation analysis was used between anosognosia index and altered FC value, brain metabolism as well as AD pathological biomarkers (Bonferroni corrected,  $p < 0.05$ ) in aMCI patients (Figure 4). The altered FC between the left OFC and the left MTG is positively correlated with anosognosia index ( $r = 0.479$ ,  $p < 0.001$ ) in in aMCI

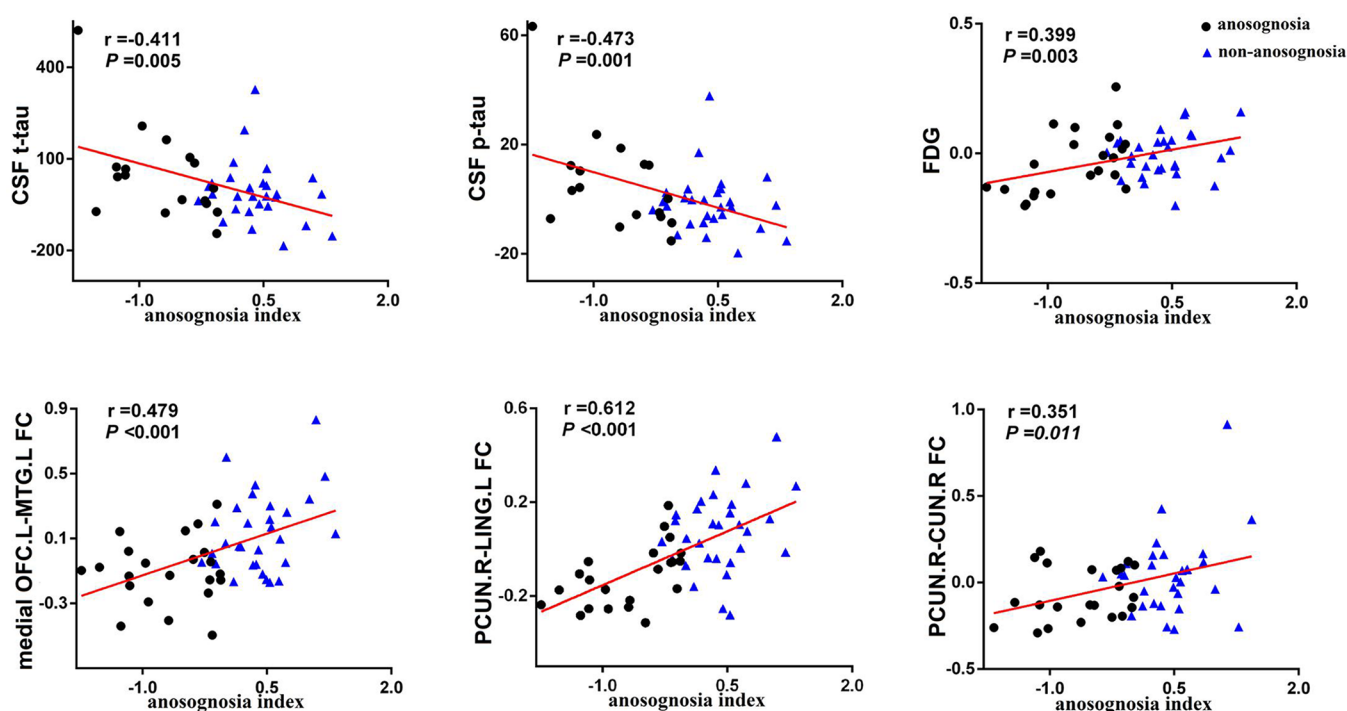


**Figure 4.** Correlations between anosognosia index and brain connectivity as well as AD biomarkers including CSF t-tau, CSF p-tau, and FDG (Bonferroni corrected,  $P < 0.05$ ). Abbreviations: CSF, cerebrospinal fluid; t-tau, total tau; p-tau, phosphorylated tau; FDG, F18-fluorodeoxyglucose; Medial OFC, medial orbitofrontal cortex; MTG, middle temporal gyrus; PCUN, precuneus; LING, lingual gyrus; CUN, cuneus; L, left; R, right.

subgroups. The changed FC between right precuneus and left lingual gyrus ( $r = 0.612$ ,  $p < 0.001$ ), as well as right cuneus ( $r = 0.351$ ,  $p = 0.011$ ), is positively correlated with anosognosia index in aMCI subgroups. These results showed significant positive associations between altered FC of medial OFC–MTG circuit as well as the precuneus–visual cortex circuit and anosognosia index in aMCI subgroups, which verified that the disruption of medial OFC–MTG circuit and the precuneus–visual cortex circuit was associated with anosognosia. In addition, we observed a positive correlation between the anosognosia index and brain glucose metabolism ( $r = 0.399$ ,  $p = 0.003$ ), negative correlation between the anosognosia index and CSF t-tau ( $r = -0.411$ ,  $p = 0.005$ ) as well as CSF p-tau ( $r = -0.473$ ,  $p = 0.001$ ) in aMCI subgroups. Age, gender, and education level were controlled in all these results. According to the research framework of A/T/N biomarker proposed by NIA-AA in 2018,<sup>54</sup> the results supported a link between anosognosia and AD neuropathology. In addition, although our results found that the CSF  $A\beta$  in aMCI with anosognosia had the tendency to decrease rapidly, there was no significant correlation between CSF  $A\beta$  and the anosognosia index. The possible reason is that CSF  $A\beta$  may not be a sensitive indicator of changed anosognosia index. This view is supported by a previous study that the evaluation of self-cognition is related to tau deposition in the elderly with normal cognition but not related to amyloid deposition.<sup>55</sup> These results revealed that the anosognosia symptom in aMCI patients is related to the dysfunction of brain intrinsic connection and AD pathological markers and emphasized the importance of evaluating anosognosia in the clinical management of aMCI patients.

**Limitations.** Although this research has some innovations, it also has some limitations. The sample size is relatively small in the study. Because the study is a longitudinal study, only

participants with demographic information, structural and functional MRI at baseline, and 2-year follow-up can be included in the study. Longitudinal large-scale study is expected in future. There are several methods for evaluating anosognosia, including patient–caregiver discrepancy scores, clinician evaluation, and subjective–objective difference scores. At present, there is no consensus on which assessment is the most appropriate method. In this study, we used the discrepancy between patient-rated score and informant-rated score to evaluate anosognosia. Because ADNI does not provide detailed information about informants, their reports may be biased. However, a previous study had reported that there is no significant difference in the informant’s characteristics between low self-awareness and heightened self-awareness groups.<sup>22</sup> Therefore, the current findings are unlikely to be confused by the prejudice of the informant.

## CONCLUSION

The present study validated a previous viewpoint that anosognosia in aMCI patients was associated with the network interruption between self-related network and memory-related network. We also found that the abnormal activity between the precuneus and visual cortex may be involved in the process of anosognosia in aMCI patients. Notably, longitudinal hyperconnectivity between left medial OFC and left MTG, right precuneus and left lingual gyrus, as well as right precuneus and right cuneus in aMCI with the anosognosia group provided a new longitudinal evolution “X” model of hypersynchronization about anosognosia, which prompted us to explore its neural mechanisms in the future. Furthermore, aMCI patients with anosognosia have severe AD pathological markers, hypometabolism, and faster clinical progression to AD dementia, which



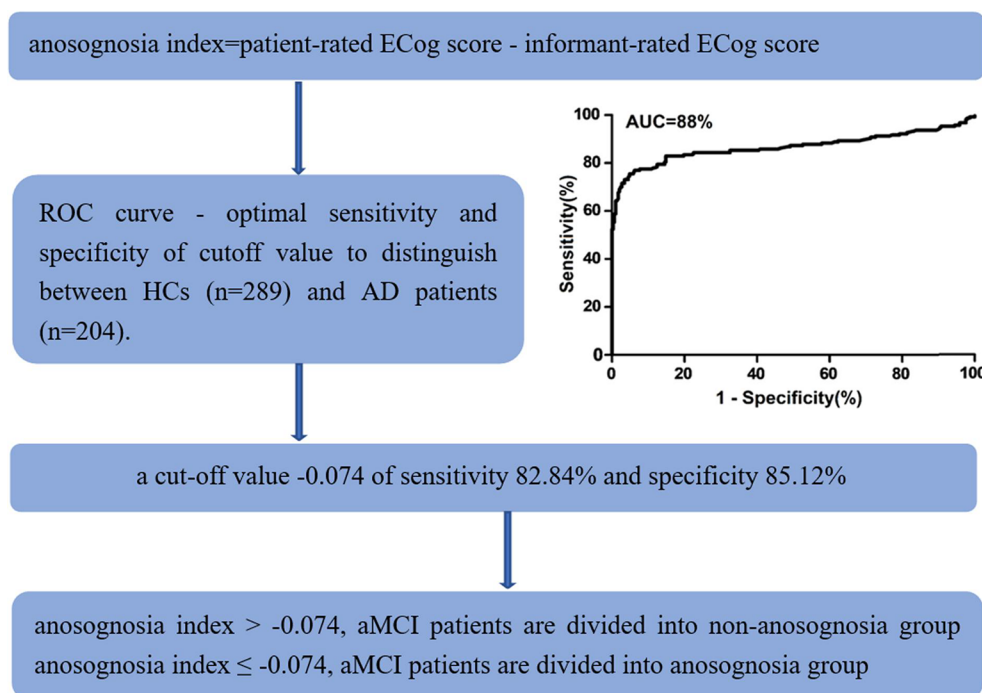


**Figure 5.** Flowchart of calculated anosognosia index and division of aMCI with anosognosia and nonanosognosia groups. Legend is adapted from the study by Theriault et al.<sup>6</sup> Abbreviations: ROC, receiver operating characteristic curve; AD, Alzheimer's disease; aMCI, amnesic mild cognitive impairment.

reminds us to pay attention to the management of anosognosia in aMCI patients.

## METHODS AND MATERIALS

**ADNI Database.** All participants in this study were obtained from the Alzheimer's Disease Neuroimaging Initiative (ADNI) database (<http://adni.loni.usc.edu>). The ADNI was launched in 2003 as a public-private partnership, led by Principal Investigator Michael W. Weiner, MD. The primary goal of ADNI has been to test whether serial magnetic resonance imaging, positron emission tomography, other biological markers, and clinical and neuropsychological assessment can be combined to measure the progression of aMCI and early AD. The ADNI recruited participants ranging from 55 to 94 years from a multicenter study conducted at 59 locations in North America.

**Participants.** Participants were recruited from the baseline period of ADNI population. All subjects had demographic information, neuropsychological scale, structural and functional MRI date for baseline, and 2-year follow-up period. The diagnostic criteria of HCs and aMCI are obtained from the ADNI Web site (<http://adni.loni.usc.edu/data-samples/access-data/>). In detail, the criteria of HCs were the following: (1) no memory complaints; (2) normal cognitive performance, Mini-Mental State Exam (MMSE) score between 24 and 30; (3) a clinical dementia rating (CDR) score equal to 0. The criteria of aMCI patients were the following: (1) memory complaints; (2) objective evidence of memory decline, a score of 0.5 on the memory part of CDR scores; (3) MMSE scores equal to 24–30 points; (4) no dementia and no signal of severe depression. On the basis of the above criteria, we identified 52 aMCI patients and 25 HCs subjects.

**Neuropsychological Assessment.** The general cognitive ability was evaluated by MoCA. Memory function was assessed by the composite score combining the Rey Auditory Verbal Learning Test, the Alzheimer Disease Assessment Scale-Cognitive, Logical Memory, and Mini-Mental State Examination. Executive function was assessed by the composite score combining Category Fluency, WAIS-R Digit Symbol, Trails A & B, Digit Span Backward, and clock drawing. We download the scale information from the ADNI Web site, and

detailed information can be obtained on the ADNI Web site (<http://adni.loni.usc.edu>).

**Evaluation of Anosognosia and Classification.** The everyday cognition (ECog) scale was applied to assess the anosognosia index consistent with a previous study.<sup>6</sup> The ECog scale<sup>56</sup> is a questionnaire combining patient-rated and informant-rated information to detect cognitive decline including six domain-specific factors (everyday memory, language, visuospatial abilities, planning, organization, and divided attention). Participants were asked to compare their current cognitive abilities with 10 years ago to measure global cognitive function. At the same time, a spouse or care giver who spent at least 10 h with the participants every week also accomplished the ECog scale based on the participants' cognitive abilities. Then, the discrepancy between patient-rated score and informant-rated score was used to determine anosognosia symptoms in the study. In previous AD spectrum studies, the application of the discrepancy score between patient-rated score and informant-rated score also proved that it was a reliable method to assess anosognosia.<sup>13,15–18</sup>

In order to obtain the cutoff value of the anosognosia index to distinguish between HCs ( $n = 289$ ) and AD patients ( $n = 204$ ) in the ADNI database, we calculated the receiver operating characteristic curve (ROC) of the anosognosia index. The cutoff values of optimal sensitivity and specificity were used to divide aMCI patients into anosognosia and nonanosognosia groups. Finally, the cutoff value  $-0.074$  (sensitivity 82.84%, specificity 85.12%) was used to divide aMCI patients into anosognosia and nonanosognosia groups. This method has been applied and reliability in previously published research.<sup>6</sup> See Figure 5 for details.

**CSF Pathological Markers.** The levels of  $A\beta$ , t-tau, and p-tau in CSF were measured by the INNO-BIAALZBio3 immunoassay reagent. Specific details can be obtained on the ADNI official Web site (<http://adni.loni.usc.edu>). Lumbar puncture is an invasive operation. Participants accept this measure voluntarily. Therefore, only part of the participants had CSF samples. In the baseline period, 62 subjects had cerebrospinal fluid sample information, including 17 HCs, 28 aMCI with nonanosognosia, and 17 aMCI patients with anosognosia. At 2 years follow-up, there were 12 HCs, 22 aMCI with nonanosognosia, and 12 aMCI with anosognosia.

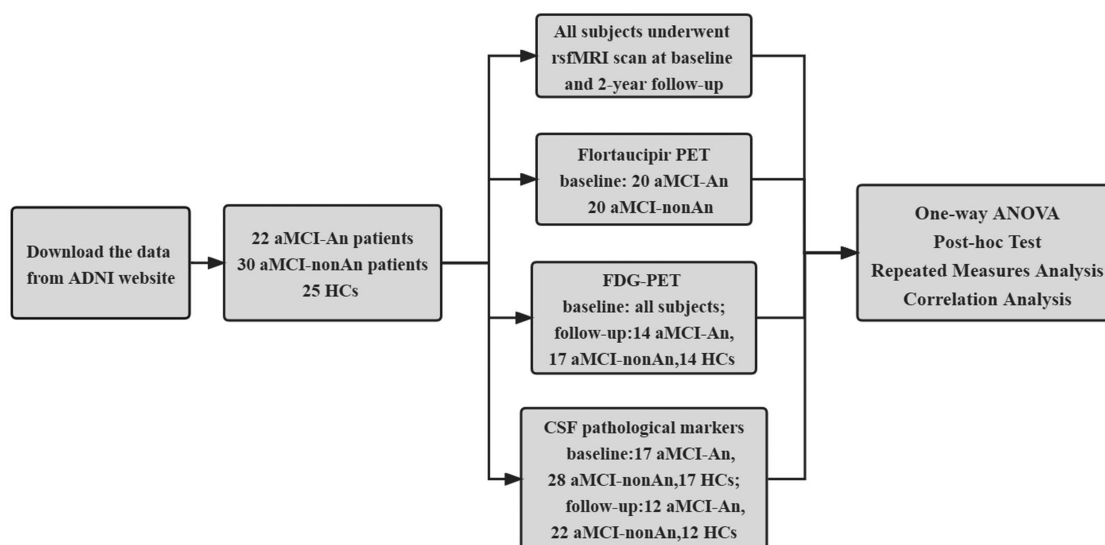


**Figure 6.** Flowchart of the number of participants in various technical modes. HCs, healthy controls; aMCI-An, aMCI with anosognosia group; aMCI-nonAn, aMCI with nonanosognosia group.

**Brain Imaging. PET.** All ADNI [ $^{18}\text{F}$ ] flortaucipir PET scans and FDG-PET were acquired following the standardized ADNI protocol for PET imaging ([adni.loni.usc.edu](http://adni.loni.usc.edu)).

**[ $^{18}\text{F}$ ]Flortaucipir PET Acquisition and Processing.** The analysis of [ $^{18}\text{F}$ ]flortaucipir PET imaging includes the flortaucipir scan and an MPRAGE for each participant that was obtained at the baseline visit as the flortaucipir image. Freesurfer (version 5.3.0) was used to segment the MPRAGE to define some regions of interest in each subject's native space. Then, the flortaucipir image is registered in its corresponding MPRAGE image that has been segmented and mean flortaucipir uptake was calculated within Freesurfer-defined regions. Mean regional uptake was calculated across Freesurfer-defined regions including cortical, subcortical, and WM regions of interest and divided by a reference region of cerebellar gray matter to generate flortaucipir standardized uptake value ratios (SUVRs). A detailed description of [ $^{18}\text{F}$ ]flortaucipir PET acquisition and processing can be found at <http://adni.loni.usc.edu/data-samples/pet/>. We downloaded the partial volume corrected SUVrs of brain regions from the ADNI file (<http://adni.loni.usc.edu>). The participants in the study voluntarily participated in [ $^{18}\text{F}$ ]flortaucipir PET scans, so not all subjects have PET data. In our study, 20 aMCI with nonanosognosia and 20 aMCI with anosognosia were scanned by [ $^{18}\text{F}$ ]flortaucipir PET.

**FDG-PET Acquisition and Processing.** The brain glucose metabolism was measured by FDG-PET in the ADNI database. The FDG-PET uptake is the average metabolic changes in the right and left angular gyri, right and left inferior temporal regions, and bilateral posterior cingulate, which are regarded as the target regions sensitive to AD and MCI (metaROIs). PET images were spatially normalized to the MNI template in Statistical Parametric Mapping 5 (SPM 5).<sup>57</sup> The average counts were extracted from the metaROIs for each subject's FDG scans at each time point, and the intensity values were computed using SPM subroutines. The mean of each metaROI was normalized by intensity by dividing by the mean of the pons/vermis reference region. The uniform spatial resolution and intensity range images were obtained by preprocessing the raw FDG-PET image data. The preprocessing steps include the following: dynamic co-registration, averaging, reorientation along the anterior–posterior commissure, filtering, and finally generated images with a full width at half-maximum (fwhm) Gaussian kernel of 8 mm  $\times$  8 mm  $\times$  8 mm.<sup>58</sup> A comprehensive presentation of FDG-PET image acquisition and preprocessing can be acquired from <http://adni.loni.usc.edu/data-samples/pet/>. All participants in the baseline period underwent FDG-PET scans. Among the participants who were followed for 2 years, 17

HCs, 17 aMCI with nonanosognosia, and 14 aMCI with anosognosia subjects underwent FDG-PET scans.

**Structural and Functional MRI. Data Acquisition.** Structural and functional MRI images were obtained on 3T scanner including Siemens (Munich, Germany), General Electric (Cleveland, OH), and Philips (Best in The Netherlands). In brief, a 3D magnetization-prepared rapid gradient-echo (MPRAGE) T1-weighted sequence with 1 mm isotropic voxel resolution and a repetition time (TR) of 2300 ms were used to recorded structural MRI. The gradient-echo echo-planar imaging (GRE-EPI) sequence was applied to obtain the fMRI images. The parameters were the following: TR = 3000 ms; echo time (TE) = 30 ms; within plane field of (FOV) = 256  $\times$  240 mm<sup>2</sup>; number of slices = 48; slice thickness = 3.3 mm; matrix = 64  $\times$  64; flip angle (FA) = 800; spatial resolution = 3.3  $\times$  3.3  $\times$  3.3 mm<sup>3</sup>.

**Image Preprocessing.** Data Processing Assistant for resting-state fMRI (DPARF, <http://restfmri.net/forum/DPARF>) and Statistical Parametric Mapping (SPM8; <http://www.fil.ion.ucl.ac.uk/spm>) were used to conduct data analyses of all groups.

**Structural MRI.** The preprocessing includes the following steps: First, the DICOM format images were converted to NIFTI format. The gray matter, white matter, and cerebrospinal fluid images were obtained by segmenting the MPRAGE images. Then, the segmented images were normalized to the Montreal Neurological Institute (MNI) standard template, voxel 1.5 mm  $\times$  1.5 mm  $\times$  1.5 mm. The gray matter map is obtained by spatial smoothing using a smoothing kernel with a fwhm of 8 mm  $\times$  8 mm  $\times$  8 mm. The obtained voxel-wise gray matter volume maps were resampled to a setting of 3  $\times$  3  $\times$  3 mm<sup>3</sup> voxels and voxel-based gray matter volume correction for subsequent analyses.

**Resting-State fMRI.** To reduce the possible instability of MRI signal, the first 10 volumes were discarded. The intravolume acquisition time differences among slices and head movement (Friston 24 parameters) effects of remaining images were corrected. Data from one aMCI patients were excluded due to the translation and rotation exceeding 3 mm and 3 $^{\circ}$ .<sup>21</sup> The fMRI images were then spatially normalized to the MNI echo-planar imaging template and resampled to a default setting (3  $\times$  3  $\times$  3 mm<sup>3</sup> voxels). Then, a 6 mm  $\times$  6 mm  $\times$  6 mm fwhm Gaussian kernel was used to reduce high spatial frequency noise.<sup>59</sup> Finally, nuisance covariate of global signal, white matter signal, and cerebrospinal fluid signal were selected to regress and filter at 0.01–0.08 Hz.<sup>59,60</sup>

This study involved multiple modes and examinations, including PET scans, AD pathology markers, and fMRI techniques, but not all subjects experienced every mode examination. Figure 6 shows the

number of subjects included in the study in PET scans, AD pathology markers, and rest state fMRI patterns.

**Statistical Analysis.** Statistical analyses were performed with Statistical Package for the Social Sciences (SPSS) software, version 22.0 (IBM, Armonk, NY, USA). The ANOVA and  $\chi^2$  test were used to measure the differences in demographic and neuropsychological scales among the three groups. The Bonferroni correction was used for pairwise comparisons. Repeated measures ANOVA was used to explore the longitudinal changes of the neuropsychological scale, pathological biomarkers (i.e.,  $A\beta$ , t-tau, and p-tau), and brain metabolism among aMCI subgroups. Pearson correlations analysis was used to examine the relationship of between anosognosia index and pathological biomarkers (i.e.,  $A\beta$ , t-tau, and p-tau) as well as brain metabolism in the aMCI subgroups. The threshold was set to  $p < 0.05$  to determine statistical significance.

We used two different imaging techniques to investigate the neural basis of anosognosia in aMCI patients. First, the two-sample  $t$  test was used to compare the tau SUVRs of freesurfer-defined regions between the aMCI with anosognosia and nonanosognosia groups. Then, Pearson correlation analysis was performed between the anosognosia index and tau SUVRs of discrepant regions obtained above to explore anosognosia-related regions. All analyses removed age, gender, and education level as covariates. In the Pearson correlation analysis, brain regions with a threshold  $p < 0.05$  were considered statistically significant and used as seeds for further seed-based FC analysis using fMRI. Specifically, we used high tau SUVRs regions as the regions of interest with 6 mm radius for voxel-wise analysis. A seed-based FC analysis was conducted by calculating the Pearson product-moment correlation coefficients between the average time course of the regions of interest and all other voxels in the GM mask of the whole brain. A one-way ANOVA was applied to compare the discrepancy of FC with high tau SUVRs regions as seeds among the three groups with age, gender, education level, and gray matter (GM) volume as covariates. Fisher's  $r$ -to- $z$  transformation was used to standardize functional map. Gaussian random field (GRF) theory was used for cluster-level multiple comparisons correction removing age, gender, education level, and GM volume as covariates ( $p < 0.05$ , corrected, two tailed). Two sample  $t$  tests were performed for post hoc comparisons, and the mask was obtained by ANOVA analysis ( $p < 0.01$ , corrected, two tailed), controlling for the effects of age, gender, education level, and GM volume.

Finally, we performed mixed effects analysis on the altered FC of aMCI with anosognosia and nonanosognosia groups to obtain the longitudinal group-time interaction among the two groups removing age, gender, education level, and GM volume as covariates ( $p < 0.01$ , corrected, two tailed). In the mixed effects model, there was an aMCI with anosognosia vs aMCI without anosognosia model as a between-subjects factor (group factors), and there was the longitudinal time as a within subject factor (time factors). Pearson correlation analysis was performed to detect the correlation between the altered FC and anosognosia index with age, gender, and education level as covariates.

## AUTHOR INFORMATION

### Corresponding Authors

**Xingjian Lin** – Department of Neurology, The Affiliated Brain Hospital of Nanjing Medical University, Nanjing, Jiangsu 210029, China; Phone: 025-82296097; Email: [linxingjian@njmu.edu.cn](mailto:linxingjian@njmu.edu.cn)

**Jiu Chen** – Institute of Neuropsychiatry, The Affiliated Brain Hospital of Nanjing Medical University, Nanjing, Jiangsu 210029, China; Institute of Brain Functional Imaging, Nanjing Medical University, Nanjing, Jiangsu 210029, China; [orcid.org/0000-0001-8185-8575](https://orcid.org/0000-0001-8185-8575); Phone: 025-82296623; Email: [ericcst@aliyun.com](mailto:ericcst@aliyun.com), [chenjiu1223@njmu.edu.cn](mailto:chenjiu1223@njmu.edu.cn)

## Authors

**Shanshan Chen** – Department of Neurology, The Affiliated Brain Hospital of Nanjing Medical University, Nanjing, Jiangsu 210029, China

**Yu Song** – Department of Neurology, The Affiliated Brain Hospital of Nanjing Medical University, Nanjing, Jiangsu 210029, China

**Huimin Wu** – Department of Neurology, The Affiliated Brain Hospital of Nanjing Medical University, Nanjing, Jiangsu 210029, China

**Honglin Ge** – Institute of Neuropsychiatry, The Affiliated Brain Hospital of Nanjing Medical University, Nanjing, Jiangsu 210029, China; Institute of Brain Functional Imaging, Nanjing Medical University, Nanjing, Jiangsu 210029, China

**Wenzhang Qi** – Department of Radiology, The Affiliated Brain Hospital of Nanjing Medical University, Nanjing, Jiangsu 210029, China

**Yue Xi** – Fourth Clinical College of Nanjing Medical University, Nanjing 211166, China

**Jiayi Wu** – Fourth Clinical College of Nanjing Medical University, Nanjing 211166, China

**Yuxiang Ji** – Fourth Clinical College of Nanjing Medical University, Nanjing 211166, China

**Xexin Chen** – Fourth Clinical College of Nanjing Medical University, Nanjing 211166, China

Complete contact information is available at:

<https://pubs.acs.org/10.1021/acschemneuro.1c00595>

## Author Contributions

\*S.C., Y.S., and H.W. contributed equally (joint first authors). S.C., Y.S., H.W., X.L., and J.C. designed the study. H.G., W.Q., Y.X., J.W., Y.J., and K.C. downloaded data and organized data. S.C., Y.S., and H.W. analyzed the data and drafted the manuscript. X.L. and J.C. modified the article and approved submission.

## Notes

The authors declare no competing financial interest.

Data used in preparation of this article were obtained from the Alzheimer's Disease Neuroimaging Initiative (ADNI) database ([adni.loni.usc.edu](http://adni.loni.usc.edu)). As such, the investigators within the ADNI contributed to the design and implementation of ADNI and/or provided data but did not participate in the analysis or writing of this report. A complete listing of ADNI investigators can be found at [http://adni.loni.usc.edu/wp-content/uploads/how\\_to\\_apply/ADNI\\_Acknowledgement\\_List.pdf](http://adni.loni.usc.edu/wp-content/uploads/how_to_apply/ADNI_Acknowledgement_List.pdf).

**Ethics Statement.** The research of ADNI was approved by the institutional review boards of each participating institution. All participants participating in the ADNI study have signed a written consent form.

## ACKNOWLEDGMENTS

This study was supported by the National Natural Science Foundation of China (Grant 81701675), Key Project supported by Medical Science and Technology Development Foundation, Nanjing Department of Health (Grant JQX18005), and Key Research and Development Plan (Social Development) Project of Jiangsu Province (Grant BE2018608). Data collection and sharing for this project were in part funded by the Alzheimer's Disease Neuroimaging Initiative (ADNI) (National Institutes of Health Grant U01 AG024904) and DOD ADNI (Department of Defense Award

W81XWH-12-2-0012). ADNI is funded by the National Institute on Aging, the National Institute of Biomedical Imaging and Bioengineering, and through generous contributions from the following: AbbVie, Alzheimer's Association; Alzheimer's Drug Discovery Foundation; Araclon Biotech; BioClinica, Inc.; Biogen; BristolMyers Squibb Company; CereSpir, Inc.; Cogstate; Eisai Inc.; Elan Pharmaceuticals, Inc.; Eli Lilly and Company; EuroImmun; F. Hoffmann-La Roche Ltd and its affiliated company Genentech, Inc.; Fujirebio; GE Healthcare; IXICO Ltd.; Janssen Alzheimer Immunotherapy Research & Development, LLC.; Johnson & Johnson Pharmaceutical Research & Development LLC.; Lumosity; Lundbeck; Merck & Co., Inc.; Meso Scale Diagnostics, LLC.; NeuroRx Research; Neurotrack Technologies; Novartis Pharmaceuticals Corporation; Pfizer Inc.; Piramal Imaging; Servier; Takeda Pharmaceutical Company; and Transition Therapeutics. The Canadian Institutes of Health Research is providing funds to support ADNI clinical sites in Canada. Private sector contributions are facilitated by the Foundation for the National Institutes of Health ([www.fnih.org](http://www.fnih.org)). The grantee organization is the Northern California Institute for Research and Education, and the study is coordinated by the Alzheimer's Therapeutic Research Institute at the University of Southern California. ADNI data are disseminated by the Laboratory for Neuro Imaging at the University of Southern California.

## REFERENCES

- (1) Starkstein, S. E.; Jorge, R.; Mizrahi, R.; Robinson, R. G. A diagnostic formulation for anosognosia in Alzheimer's disease. *J. Neurol., Neurosurg. Psychiatry* **2006**, *77*, 719–725.
- (2) Ott, B. R.; Lafleche, G.; Whelihan, W. M.; Buongiorno, G. W.; Albert, M. S.; Fogel, B. S. Impaired awareness of deficits in Alzheimer disease. *Alzheimer Dis. Assoc. Disord.* **1996**, *10*, 68–76.
- (3) Langa, K. M.; Levine, D. A. The diagnosis and management of mild cognitive impairment: a clinical review. *JAMA* **2014**, *312*, 2551–2561.
- (4) Mondragon, J. D.; Maurits, N. M.; De Deyn, P. P. Functional Neural Correlates of Anosognosia in Mild Cognitive Impairment and Alzheimer's Disease: a Systematic Review. *Neuropsychol Rev.* **2019**, *29*, 139–165.
- (5) Gerretsen, P.; Chung, J. K.; Shah, P.; Plitman, E.; Iwata, Y.; Caravaggio, F.; Nakajima, S.; Pollock, B. G.; Graff-Guerrero, A. Anosognosia Is an Independent Predictor of Conversion From Mild Cognitive Impairment to Alzheimer's Disease and Is Associated With Reduced Brain Metabolism. *J. Clin. Psychiatry* **2017**, *78*, e1187–e1196 (Alzheimer's Disease Neuroimaging I).
- (6) Theriault, J.; Ng, K. P.; Pascoal, T. A.; Mathotaarachchi, S.; Kang, M. S.; Struyfs, H.; Shin, M.; Benedet, A. L.; Walpol, I. C.; Nair, V.; Gauthier, S.; Rosa-Neto, P. Anosognosia predicts default mode network hypometabolism and clinical progression to dementia. *Neurology* **2018**, *90*, e932–e939.
- (7) Vannini, P.; Hanseeuw, B.; Munro, C. E.; Amariglio, R. E.; Marshall, G. A.; Rentz, D. M.; Pascual-Leone, A.; Johnson, K. A.; Sperling, R. A. Anosognosia for memory deficits in mild cognitive impairment: Insight into the neural mechanism using functional and molecular imaging. *Neuroimage Clin* **2017**, *15*, 408–414.
- (8) Valera-Bermejo, J. M.; De Marco, M.; Mitolo, M.; McGeown, W. J.; Venneri, A. Neuroanatomical and cognitive correlates of domain-specific anosognosia in early Alzheimer's disease. *Cortex* **2020**, *129*, 236–246.
- (9) Guerrier, L.; Le Men, J.; Gane, A.; Planton, M.; Salabert, A. S.; Payoux, P.; Dumas, H.; Bonneville, F.; Péran, P.; Pariente, J. Involvement of the Cingulate Cortex in Anosognosia: A Multimodal Neuroimaging Study in Alzheimer's Disease Patients. *J. Alzheimer's Dis.* **2018**, *65*, 443–453.
- (10) Bregman, N.; Kavé, G.; Zeltzer, E.; Biran, I. Memory impairment and Alzheimer's disease pathology in individuals with MCI who underestimate or overestimate their decline. *Int. J. Geriatr Psychiatry* **2020**, *35*, 581–588.
- (11) Perrotin, A.; Desgranges, B.; Landeau, B.; Mezenge, F.; La Joie, R.; Egret, S.; Pelerin, A.; de la Sayette, V.; Eustache, F.; Chetelat, G. Anosognosia in Alzheimer disease: Disconnection between memory and self-related brain networks. *Ann. Neurol.* **2015**, *78*, 477–486.
- (12) Antoine, N.; Bahri, M. A.; Bastin, C.; Collette, F.; Phillips, C.; Balteau, E.; Genon, S.; Salmon, E. Anosognosia and default mode subnetwork dysfunction in Alzheimer's disease. *Human Brain Mapping* **2019**, *40*, 5330–5340.
- (13) Ries, M. L.; Jabbar, B. M.; Schmitz, T. W.; Trivedi, M. A.; Gleason, C. E.; Carlsson, C. M.; Rowley, H. A.; Asthana, S.; Johnson, S. C. Anosognosia in mild cognitive impairment: Relationship to activation of cortical midline structures involved in self-appraisal. *J. Int. Neuropsychol. Soc.* **2007**, *13*, 450–461.
- (14) Gaubert, M.; Villain, N.; Landeau, B.; Mezenge, F.; Egret, S.; Perrotin, A.; Belliard, S.; de La Sayette, V.; Eustache, F.; Desgranges, B.; Chetelat, G.; Rauchs, G. Neural Correlates of Self-Reference Effect in Early Alzheimer's Disease. *J. Alzheimer's Dis.* **2017**, *56*, 717–731.
- (15) Hanseeuw, B. J.; Scott, M. R.; Sikkes, S. A. M.; Properi, M.; Gatchel, J. R.; Salmon, E.; Marshall, G. A.; Vannini, P. Evolution of anosognosia in Alzheimer's disease and its relationship to amyloid. *Ann. Neurol.* **2020**, *87*, 267–280 (Alzheimer's Disease Neuroimaging I).
- (16) Cacciamani, F.; Sambati, L.; Houot, M.; Habert, M. O.; Dubois, B.; Epelbaum, S. Awareness of cognitive decline trajectories in asymptomatic individuals at risk for AD. *Alzheimers Res. Ther* **2020**, *12*, 129 (Group IN-Ps).
- (17) Vannini, P.; Hanseeuw, B. J.; Gatchel, J. R.; Sikkes, S. A. M.; Alzate, D.; Zuluaga, Y.; Moreno, S.; Mendez, L.; Baena, A.; Ospina-Lopera, P.; Tirado, V.; Henao, E.; Acosta-Baena, N.; Giraldo, M.; Lopera, F.; Quiroz, Y. T. Trajectory of Unawareness of Memory Decline in Individuals With Autosomal Dominant Alzheimer Disease. *JAMA Netw Open* **2020**, *3*, No. e2027472.
- (18) Mondragon, J. D.; Maurits, N. M.; De Deyn, P. P. Functional connectivity differences in Alzheimer's disease and amnesic mild cognitive impairment associated with AT(N) classification and anosognosia. *Neurobiol. Aging* **2021**, *101*, 22–39 (Alzheimer's Disease Neuroimaging I).
- (19) Tagai, K.; Shinagawa, S.; Kada, H.; Inamura, K.; Nagata, T.; Nakayama, K. Anosognosia in mild Alzheimer's disease is correlated with not only neural dysfunction but also compensation. *Psychogeriatrics* **2018**, *18*, 81–88.
- (20) Ossenkoppele, R.; Rabinovici, G. D.; Smith, R.; Cho, H.; Scholl, M.; Strandberg, O.; Palmqvist, S.; Mattsson, N.; Janelidze, S.; Santillo, A.; Ohlsson, T.; Jogi, J.; Tsai, R.; La Joie, R.; Kramer, J.; Boxer, A. L.; Gorno-Tempini, M. L.; Miller, B. L.; Choi, J. Y.; Ryu, Y. H.; Lyoo, C. H.; Hansson, O. Discriminative Accuracy of [<sup>18</sup>F]-flortaucipir Positron Emission Tomography for Alzheimer Disease vs Other Neurodegenerative Disorders. *JAMA* **2018**, *320*, 1151–1162.
- (21) Chen, S.; Song, Y.; Xu, W.; Hu, G.; Ge, H.; Xue, C.; Gao, J.; Qi, W.; Lin, X.; Chen, J. Impaired Memory Awareness and Loss Integration in Self-Referential Network Across the Progression of Alzheimer's Disease Spectrum. *J. Alzheimer's Dis.* **2021**, *83*, 111–126 (Alzheimer's Disease Neuroimaging I).
- (22) Cacciamani, F.; Tandetnik, C.; Gagliardi, G.; Bertin, H.; Habert, M. O.; Hampel, H.; Boukadida, L.; Revillon, M.; Epelbaum, S.; Dubois, B. Low Cognitive Awareness, but Not Complaint, is a Good Marker of Preclinical Alzheimer's Disease. *J. Alzheimer's Dis.* **2017**, *59*, 753–762 (Group IN-PS).
- (23) McDonough, I. M.; Cervantes, S. N.; Gray, S. J.; Gallo, D. A. Memory's aging echo: age-related decline in neural reactivation of perceptual details during recollection. *NeuroImage* **2014**, *98*, 346–358.
- (24) Edmonds, E. C.; Delano-Wood, L.; Galasko, D. R.; Salmon, D. P.; Bondi, M. W. Subjective cognitive complaints contribute to

- misdiagnosis of mild cognitive impairment. *J. Int. Neuropsychol. Soc.* **2014**, *20*, 836–847 (Alzheimer's Disease Neuroimaging I).
- (25) Wilson, R. S.; Boyle, P. A.; Yu, L.; Barnes, L. L.; Sytsma, J.; Buchman, A. S.; Bennett, D. A.; Schneider, J. A. Temporal course and pathologic basis of unawareness of memory loss in dementia. *Neurology* **2015**, *85*, 984–991.
- (26) Munro, C. E.; Donovan, N. J.; Amariglio, R. E.; Papp, K. V.; Marshall, G. A.; Rentz, D. M.; Pascual-Leone, A.; Sperling, R. A.; Locascio, J. J.; Vannini, P. The Impact of Awareness of and Concern About Memory Performance on the Prediction of Progression From Mild Cognitive Impairment to Alzheimer Disease Dementia. *Am. J. Geriatr Psychiatry* **2018**, *26*, 896–904.
- (27) Hallam, B.; Chan, J.; Gonzalez Costafreda, S.; Bhome, R.; Huntley, J. What are the neural correlates of meta-cognition and anosognosia in Alzheimer's disease? A systematic review. *Neurobiol. Aging* **2020**, *94*, 250–264.
- (28) Michon, A.; Deweer, B.; Pillon, B.; Agid, Y.; Dubois, B. Relation of anosognosia to frontal lobe dysfunction in Alzheimer's disease. *J. Neurol., Neurosurg. Psychiatry* **1994**, *57*, 805–809.
- (29) Sedaghat, F.; Dedousi, E.; Baloyannis, I.; Tegos, T.; Costa, V.; Dimitriadis, A. S.; Baloyannis, S. J. Brain SPECT findings of anosognosia in Alzheimer's disease. *J. Alzheimer's Dis.* **2010**, *21*, 641–647.
- (30) Riga, D.; Matos, M. R.; Glas, A.; Smit, A. B.; Spijker, S.; Van den Oever, M. C. Optogenetic dissection of medial prefrontal cortex circuitry. *Front. Syst. Neurosci.* **2014**, *8*, 230.
- (31) Nogueira, R.; Abolafia, J. M.; Drugowitsch, J.; Balaguer-Balaster, E.; Sanchez-Vives, M. V.; Moreno-Bote, R. Lateral orbitofrontal cortex anticipates choices and integrates prior with current information. *Nat. Commun.* **2017**, *8*, 14823.
- (32) Davey, C. G.; Pujol, J.; Harrison, B. J. Mapping the self in the brain's default mode network. *NeuroImage* **2016**, *132*, 390–397.
- (33) Xue, C.; Yuan, B.; Yue, Y.; Xu, J.; Wang, S.; Wu, M.; Ji, N.; Zhou, X.; Zhao, Y.; Rao, J.; Yang, W.; Xiao, C.; Chen, J. Distinct Disruptive Patterns of Default Mode Subnetwork Connectivity Across the Spectrum of Preclinical Alzheimer's Disease. *Front. Aging Neurosci.* **2019**, *11*, 307.
- (34) Leech, R.; Sharp, D. J. The role of the posterior cingulate cortex in cognition and disease. *Brain* **2014**, *137*, 12–32.
- (35) Krause, B. J.; Schmidt, D.; Mottaghy, F. M.; Taylor, J.; Halsband, U.; Herzog, H.; Tellmann, L.; Muller-Gartner, H. W. Episodic retrieval activates the precuneus irrespective of the imagery content of word pair associates. A PET study. *Brain* **1999**, *122* (2), 255–263.
- (36) Cavanna, A. E.; Trimble, M. R. The precuneus: a review of its functional anatomy and behavioural correlates. *Brain* **2006**, *129*, 564–583.
- (37) Whitfield-Gabrieli, S.; Moran, J. M.; Nieto-Castanon, A.; Triantafyllou, C.; Saxe, R.; Gabrieli, J. D. Associations and dissociations between default and self-reference networks in the human brain. *NeuroImage* **2011**, *55*, 225–232.
- (38) Gillihan, S. J.; Farah, M. J. Is self special? A critical review of evidence from experimental psychology and cognitive neuroscience. *Psychol. Bull.* **2005**, *131*, 76–97.
- (39) Northoff, G.; Bermpohl, F. Cortical midline structures and the self. *Trends Cognit. Sci.* **2004**, *8*, 102–107.
- (40) Northoff, G.; Heinzel, A.; de Greck, M.; Bermpohl, F.; Dobrowolny, H.; Panksepp, J. Self-referential processing in our brain—a meta-analysis of imaging studies on the self. *NeuroImage* **2006**, *31*, 440–457.
- (41) Churchland, P. S. Self-representation in nervous systems. *Science* **2002**, *296*, 308–310.
- (42) Chao, O. Y.; de Souza Silva, M. A.; Yang, Y. M.; Huston, J. P. The medial prefrontal cortex - hippocampus circuit that integrates information of object, place and time to construct episodic memory in rodents: Behavioral, anatomical and neurochemical properties. *Neurosci. Biobehav. Rev.* **2020**, *113*, 373–407.
- (43) Bogousslavsky, J.; Miklossy, J.; Deruaz, J. P.; Assal, G.; Regli, F. Lingual and fusiform gyri in visual processing: a clinico-pathologic study of superior altitudinal hemianopia. *J. Neurol., Neurosurg. Psychiatry* **1987**, *50*, 607–614.
- (44) Zhang, L.; Qiao, L.; Chen, Q.; Yang, W.; Xu, M.; Yao, X.; Qiu, J.; Yang, D. Gray Matter Volume of the Lingual Gyrus Mediates the Relationship between Inhibition Function and Divergent Thinking. *Front. Psychol.* **2016**, *7*, 1532.
- (45) Ghandili, M.; Munakomi, S. Neuroanatomy, Putamen. In *StatPearls*; StatPearls Publishing: Treasure Island, FL, 2020.
- (46) Vinas-Guasch, N.; Wu, Y. J. The role of the putamen in language: a meta-analytic connectivity modeling study. *Brain Struct. Funct.* **2017**, *222*, 3991–4004.
- (47) Rajah, M. N.; Languay, R.; Grady, C. L. Age-related changes in right middle frontal gyrus volume correlate with altered episodic retrieval activity. *J. Neurosci.* **2011**, *31*, 17941–17954.
- (48) Carter, R. M.; O'Doherty, J. P.; Seymour, B.; Koch, C.; Dolan, R. J. Contingency awareness in human aversive conditioning involves the middle frontal gyrus. *NeuroImage* **2006**, *29*, 1007–1012.
- (49) Jakabek, D.; Power, B. D.; Macfarlane, M. D.; Walterfang, M.; Velakoulis, D.; van Westren, D.; Latt, J.; Nilsson, M.; Looi, J. C. L.; Santillo, A. F. Regional structural hypo- and hyperconnectivity of frontal-triangular and frontal-thalamic pathways in behavioral variant frontotemporal dementia. *Hum Brain Mapp* **2018**, *39*, 4083–4093.
- (50) Fujimoto, H.; Matsuoka, T.; Kato, Y.; Shibata, K.; Nakamura, K.; Yamada, K.; Narumoto, J. Brain regions associated with anosognosia for memory disturbance in Alzheimer's disease: a magnetic resonance imaging study. *Neuropsychiatr. Dis. Treat.* **2017**, *13*, 1753–1759.
- (51) Pusil, S.; Lopez, M. E.; Cuesta, P.; Bruna, R.; Pereda, E.; Maestu, F. Hypersynchronization in mild cognitive impairment: the 'X' model. *Brain* **2019**, *142*, 3936–3950.
- (52) Mashour, G. A.; Frank, L.; Batthyany, A.; Kolanowski, A. M.; Nahm, M.; Schulman-Green, D.; Greyson, B.; Pakhomov, S.; Karlawish, J.; Shah, R. C. Paradoxical lucidity: A potential paradigm shift for the neurobiology and treatment of severe dementias. *Alzheimer's Dementia* **2019**, *15*, 1107–1114.
- (53) Bonanni, L.; Moretti, D.; Benussi, A.; Ferri, L.; Russo, M.; Carrarini, C.; Barbone, F.; Arnaldi, D.; Falasca, N. W.; Koch, G.; Cagnin, A.; Nobili, F.; Babiloni, C.; Borroni, B.; Padovani, A.; Onofri, M.; Franciotti, R. Hyperconnectivity in Dementia Is Early and Focal and Wanes with Progression. *Cereb Cortex* **2021**, *31*, 97–105 (Group SINDEM FTDis).
- (54) Jack, C. R.; Bennett, D. A.; Blennow, K.; Carrillo, M. C.; Dunn, B.; Haeblerlein, S. B.; Holtzman, D. M.; Jagust, W.; Jessen, F.; Karlawish, J.; Liu, E.; Molinuevo, J. L.; Montine, T.; Phelps, C.; Rankin, K. P.; Rowe, C. C.; Scheltens, P.; Siemers, E.; Snyder, H. M.; Sperling, R.; Elliott, C.; Masliah, E.; Ryan, L.; Silverberg, N. NIA-AA Research Framework: Toward a biological definition of Alzheimer's disease. *Alzheimer's Dementia* **2018**, *14*, 535–562.
- (55) d'Oleire Uquillas, F.; Jacobs, H. I. L.; Schultz, A. P.; Hanseeuw, B. J.; Buckley, R. F.; Sepulcre, J.; Pascual-Leone, A.; Donovan, N. J.; Johnson, K. A.; Sperling, R. A.; Vannini, P. Functional and Pathological Correlates of Judgments of Learning in Cognitively Unimpaired Older Adults. *Cereb Cortex* **2020**, *30*, 1974–1983.
- (56) Farias, S. T.; Mungas, D.; Reed, B. R.; Cahn-Weiner, D.; Jagust, W.; Baynes, K.; DeCarli, C. Supplemental Material for The Measurement of Everyday Cognition (ECog): Scale Development and Psychometric Properties. *Neuropsychology* **2008**, *22*, 531–544.
- (57) Yu, G. X.; Zhang, T.; Hou, X. H.; Ou, Y. N.; Hu, H.; Wang, Z. T.; Guo, Y.; Xu, W.; Tan, L.; Yu, J. T.; Tan, L. Associations of Vascular Risk with Cognition, Brain Glucose Metabolism, and Clinical Progression in Cognitively Intact Elders. *J. Alzheimer's Dis.* **2021**, *80*, 321–330 (Alzheimer's Disease Neuroimaging I).
- (58) Ou, Y. N.; Xu, W.; Li, J. Q.; Guo, Y.; Cui, M.; Chen, K. L.; Huang, Y. Y.; Dong, Q.; Tan, L.; Yu, J. T. FDG-PET as an independent biomarker for Alzheimer's biological diagnosis: a longitudinal study. *Alzheimer's Res. Ther.* **2019**, *11*, 57 (Alzheimer's Disease Neuroimaging I).
- (59) Xue, C.; Sun, H.; Yue, Y.; Wang, S.; Qi, W.; Hu, G.; Ge, H.; Yuan, Q.; Rao, J.; Tian, L.; Xiao, C.; Chen, J. Structural and

Functional Disruption of Salience Network in Distinguishing Subjective Cognitive Decline and Amnesic Mild Cognitive Impairment. *ACS Chem. Neurosci.* **2021**, *12*, 1384–1394.

(60) Chen, J.; Ma, N.; Hu, G.; Nousayhah, A.; Xue, C.; Qi, W.; Xu, W.; Chen, S.; Rao, J.; Liu, W.; Zhang, F.; Zhang, X. rTMS modulates precuneus-hippocampal subregion circuit in patients with subjective cognitive decline. *Aging* **2021**, *13*, 1314–1331.

**JACS** Au  
AN OPEN ACCESS JOURNAL OF THE AMERICAN CHEMICAL SOCIETY

Editor-in-Chief  
**Prof. Christopher W. Jones**  
Georgia Institute of Technology, USA

**Open for Submissions**

pubs.acs.org/jacsau ACS Publications  
Most Trusted. Most Cited. Most Read.